Materials Today Bio 21 (2023) 100698

Contents lists available at ScienceDirect

Materials Today Bio

journal homepage: www.journals.elsevier.com/materials-today-bio

Self-assembly nanoplatform of platinum (IV) prodrug for enhanced ovarian cancer therapy

Xiao Ma [a,b,1], Yangjia Liu [c,d,1], Hanmei Wu [a], Jinxiu Tan [a], Wenying Yi [a], Zhenjie Wang [e,**], Zhiqiang Yu [d,f,*], Xuefeng Wang [a,***]

[a] Department of Obstetrics and Gynecology, Third Affiliated Hospital, Southern Medical University, Guangzhou, 510630, PR China
[b] Department of Obstetrics and Gynecology, Guangdong Provincial People's Hospital (Guangdong Academy of Medical Sciences), Southern Medical University, Guangzhou, 510080, PR China
[c] Department of Medicine and Health Technology and Engineering, Shenzhen Bay Laboratory, Shenzhen, 518067, PR China
[d] Department of Pharmacy, Southern Medical University, Guangzhou, 510515, PR China
[e] The People's Hospital of Gaozhou, Maoming, 525200, PR China
[f] Department of Laboratory Medicine, Dongguan Institute of Clinical Cancer Research, Affiliated Dongguan Hospital, Southern Medical University, Dongguan, 523018, PR China

ARTICLE INFO

Keywords:
Cisplatin
COX-2 inhibitor
Tolfenamic acid
Synergistic therapy
Nanoprodrug

ABSTRACT

Cisplatin is a metal platinum complex commonly used in the field of anti-tumor and one of the most commonly used drugs in combination chemotherapy. However, chemotherapy with Cisplatin induced overexpression of cyclooxygenase-2 (COX-2) protein in tumor cells, which could impair the therapeutic effect of chemotherapy on tumor progression. Here, we presented a novel method for the treatment of ovarian cancer with a self-assembly based nano-system. Cisplatin and tolfenamic acid were each linked to linoleic acid to give them the ability to self-assemble into nanoparticles in water. TPNPs had flexible drug ratio adjustability, homogeneous stability, and high drug loading capacity. Compared with Cisplatin, TPNPs could promote cellular uptake and tumor aggregation, co-induce enhanced apoptosis and tumor growth inhibition by inhibiting COX-2 in the mice xenograft model of human ovarian cancer, and reduce systemic toxicity. Therefore, TPNPs is a promising antitumor drug as a kind of self-assembly nano-prodrug with high drug load.

1. Introduction

Ovarian cancer has the second highest mortality rate in gynecological cancers [1]. Surgery and platinum-based chemotherapy remain the primary means of treatment [2,3]. Up to now, Cisplatin has a very clear benefit to ovarian cancer patients and plays an important part in the modern treatment [4,5]. Despite its effectiveness, it could cause serious side effects in normal and healthy tissues, especially renal toxicity [6–8]. In this era of precision medicine, nanomedicine is being widely studied to reduce the limitations of free drug [9]. The application of nanomedicine could be very flexible, diverse and effective, such as reducing toxic and side effects through the response of microenvironment in specific parts of the body [10], enhancing penetration through bio-membrane encapsulation [11,12], and achieving painless treatment in combination with minimally invasive therapies [13]. Recent studies have shown that some platinum-based nano-carriers have been able to markedly reverse these adverse effects [14–16]. Self-assembly of nano-platinum drugs is a promising strategy for reducing drug toxicity while maintaining pharmacological efficacy [17–19]. This platform combines several advantages, such as simple preparation method, high drug loading, stability and safety, which represents a prospective anti-cancer approach. Therefore, the strategy of modifying Cisplatin into self-assembling prodrug is very feasible and significant (see Scheme 1).

Unfortunately, Cisplatin induced apoptosis was accompanied by increased cyclooxygenase-2 (COX-2) expression [20], which seemed to be involved in various steps of tumor progression and malignant

* Corresponding author. Department of Pharmacy, Southern Medical University, Guangzhou, 510515, PR China.
** Corresponding author. The People's Hospital of Gaozhou, Maoming, 525200, PR China.
*** Corresponding author. Department of Obstetrics and Gynecology, Third Affiliated Hospital, Southern Medical University, Guangzhou, 510630, PR China.
E-mail addresses: gzmaxiao0106@163.com (X. Ma), 1850072928@qq.com (Y. Liu), 934517035@qq.com (H. Wu), tanjinxiufighting@163.com (J. Tan), 350988539@qq.com (W. Yi), zhenjie55@qq.com (Z. Wang), yuzq@smu.edu.cn (Z. Yu), douwangxuefeng@163.com (X. Wang).
[1] These authors contributed equally to this work.

https://doi.org/10.1016/j.mtbio.2023.100698
Received 22 March 2023; Received in revised form 22 May 2023; Accepted 7 June 2023
Available online 17 June 2023

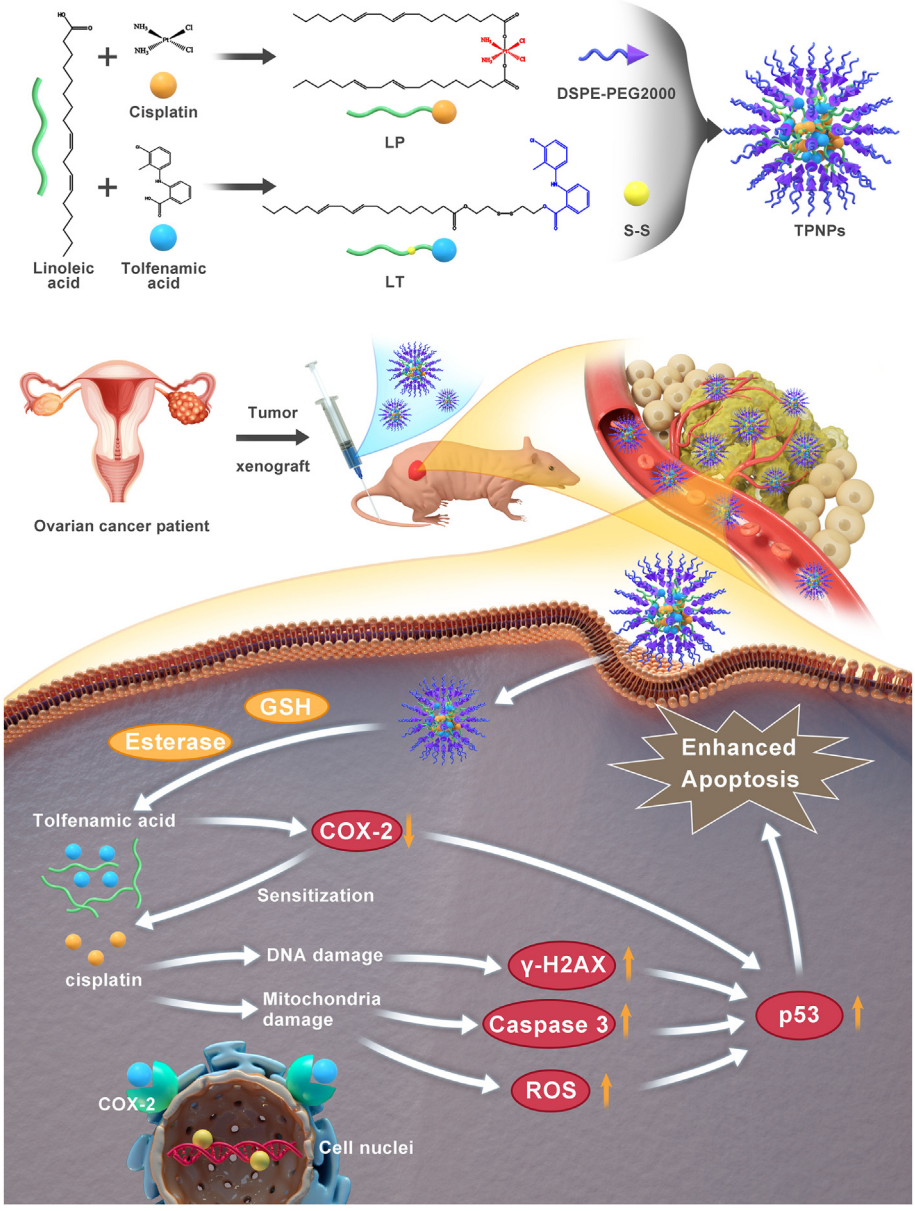

Scheme 1. Schematic drawing of TPNPs preparation and their possible mechanism *in vivo*.

transformation [21]. Recently, COX-2 has been found to participates in the development of ovarian cancer through multiple mechanisms. The overexpression of COX-2 has been linked to decreased apoptosis, increased proliferation, and angiogenesis, which might be an independent risk factor for the poor overall survival of ovarian cancer [22,23]. According to previous report, COX-2 inhibition could potentiate the anti-tumor activity of Cisplatin without increasing toxicity *in vivo* [24]. Tolfenamic acid (Tolf) is a COX-2 inhibitor with high biosafety and selectivity. In recent years, some studies have confirmed that Tolf can induce apoptosis of cancer cells and suppress the occurrence and growth of various types of cancer, especially in ovarian cancer [25–27]. Furthermore, the combination of Tolf and other agents, such as Cisplatin, Curcumin, and metal complexes, has shown synergistic antitumor effects [28–30]. Thus, we selected the combination of Tolf and Cisplatin to improve the therapeutic efficacy of ovarian cancer.

On the basis of former research, the self-aggregation system of platinum (II)-Tolf could increase the drug concentration in tumors and obtain better anti-tumor effects [31,32]. But the 1:1 ratio was immutable and the resulting synergies were not widely applicable to more types of cancers. Here, we attempted to link two hydrophobic toxic anticancer drugs to unsaturated fatty acids and give them the ability to self-assemble into nanoparticles (NPs) for synergistic treatment of ovarian cancer. The combination index of Cisplatin and Tolf on A2780 cells was measured to determine the optimal ratio of NPs (named TPNPs). When administered intravenously, TPNPs could prolong blood circulation and passively accumulate into tumor through the enhanced permeability and retention (EPR) effect. After phagocytosis, TPNPs hydrolyzes under the condition of esterase and high glutathione (GSH) content in tumor cells and releases free Cisplatin hydrate and Tolf, playing synergistic anti-tumor effects at the same time.

2. Materials and methods

2.1. Materials

Cisplatin was provided by Macklin Biotech Co., Ltd (Shanghai, China). Tolf was acquired from Yuanye Biotech Co., Ltd (Shanghai, China). Linoleic acid (LA) was purchased from Zesheng Biotech Co., Ltd

(Shanghai, China). 4-Dimethylaminopyridine (DMAP) and 1-(3-Dimethylaminopropyl)-3-ethylcarbodiimide hydrochloride (EDC) were provided by Bide Medical Technology Co., Ltd (Shanghai, China). 2-Hydroxyethyl disulfide was acquired from Meryer Biotech Co., Ltd (Shanghai, China). DSPEG-PEG2000 was provided by AVT Pharmaceutical Technology Co., Ltd (Shanghai, China).

A2780 tumor cells and Ovarian cancer patient-derived xenograft (PDX) tumor blocks were acquired from the Institute of Applied Chemistry, CAS (Changchun, China). Roswell Park Memorial Institute (RPMI-1640), Fetal bovine serum, trypsin and penicillin-streptomycin were provided by Gibco (Beijing, China). MTT, Annexin V-FITC/Propidium Iodide (FITC/PI) Apoptosis Detection Kit, Reactive Oxygen Species Detection Kit, Hoechst 33,342 and Cy5.5 were obtained from Beyotime Biotech Co., Ltd (Shanghai, China). The reagents were of analytical grade.

2.2. Animals

BALB/c female nude mice (18–20 g) aged 6–8 weeks were provided by Guangdong Medical Laboratory Animal Center. All animal experiments were conducted in accordance with those protocols ratified by the Animal Laboratory Center of Southern Medical University.

2.3. Synthesis of prodrugs

2.3.1. Synthesis of LP

Cisplatin (0.50 g, 1.68 mmol), deionized water (10 mL) and H2O2 (10 mL) was mixed and stirred for 24 h. Then the oxidized Cisplatin was collected through freeze-dried technology. LA (1.41 g, 5.04 mmol), DMAP (0.062 g, 0.51 mmol) and EDC (1.45 g, 7.56 mmol) was added into anhydrous dichloromethane (DCM) (20 mL), stirred for 15 min in an ice water bath. Afterwards, oxidized Cisplatin was added into it and stirred for 12 h at a room temperature. Then ethanol was removed by rotary evaporation under reduced pressure in a water bath at 60 °C. Eventually, the residue was purified with nonpolar solvent (Petroleum ether: Ethyl acetate = 20:1) in silica gel column chromatography to give the final product (LP) as a yellow oily liquid. Then LP was characterized by Hydrogen nuclear magnetic resonance spectroscopy (^{1}H NMR, Bruker 400, 400 MHz) and Electrospray ionization mass spectrometry (ESI-MS, Q Exactive, Thermofisher).

2.3.2. Synthesis of LT

Tolf (0.50 g, 1.91 mmol), DMAP (0.025 g, 0.21 mmol) and EDC (0.55 g, 2.87 mmol) were added into anhydrous DCM (10 mL), stirred for 15 min in an ice water bath. Afterwards, 2-hydroxyethyl disulfide (0.44 g, 2.87 mmol) was mixed into it and stirred for 12 h at a room temperature. Next, the subsequent operations were as shown in 2.3.1. The intermediate product was firstly prepared. Similarly, LA (0.52 g, 1.86 mmol), DMAP (0.022 g, 0.18 mmol) and EDC (0.53 g, 2.79 mmol) was added into anhydrous DCM (10 mL), stirred for 15 min in an ice water bath. Afterwards, the intermediate product was added and stirred for 12 h at a room temperature. Finally, the same process was used to obtain the final product (LT). Then LT was characterized by ^{1}H NMR and ESI-MS.

2.4. Preparation of TPNPs

LT, LP and DSPEG-PEG2000 were dissolved in DMF of 0.1 mL, with a mass ratio of 15:5:1. Then it was quickly added to 0.9 mL of phosphate buffered solution (PBS) under the vortex oscillation. Finally, the solution was put into the dialysis bag (MWCO 3500 Da) and the organic solvent was removed by dialysis overnight. PNPs and TNPs were prepared by the same method. The contents of Pt were determined by ICP-MS (NexION 2000, Perkin Elmer). The contents of Tolf and LT were measured by reversed phase high performance liquid chromatography (RP-HPLC). The chromatogram was performed on a reverse ODS Cosmosil-C18 column (250 mm × 4.6 mm, 5 μm) with mobile phases consisting of H_2O and Acetonitrile (10:90, V/V) at the velocity of 1.0 mL/min (290 nm).

2.5. Characterization of TPNPs

2.5.1. Determination of dimension, zeta potential and morphology

Zetasizer (Nano-ZS90, Malvern, UK) was employed to determine the dimension of TNPs, PNPs and TPNPs. The assay was duplicated three times for each sample. The negative staining method was used to display the morphology of three NPs. Specifically, NPs were firstly dripped on a copper grid and the filter paper was applied to blot the excess surrounding fluid. Then it was dried at 37 °C and stained with 2% phosphortungstic acid. Finally, the morphology was characterized by the transmission electron microscopy (TEM, Hitachi, Japan).

2.5.2. Drug release in vitro

The drug release *in vitro* was investigated by dialysis and used to evaluate drug release behavior *in vivo*. Primarily, the release medium was prepared by PBS (pH 7.4) and PBS (pH 7.4) with 10 mM glutathione (GSH). 1% Tween 80 was mixed in the release medium and employed to increase the drug solubility. The dialysis bag (MWCO 3500 Da) was activated in boiled water for 10 min. TPNPs (2 mL) were added into the prepared dialysis bag. Then the dialysis bag was placed in different release medium (20 mL) and placed in the shaker, stirred at 100 rpm. Three duplicates were repeated for each group. When the predetermined time (0.5, 1, 2, 4, 8, 12, 24 h) was arrived, the medium (0.8 mL) was removed from the dialyzer, followed by addition of an equal amount of fresh release medium was supplemented. The quantity of Tolf was determined by the HPLC. The contents of Pt were determined by ICP-MS. The drug release curves of TNPs and PNPs were determined by the same method.

2.6. Cell culture

The A2780 cells were incubated in an RMPI 1640 medium with 10% FBS and 1% penicillin-streptomycin at 37 °C in a sterile incubator containing 5% CO_2.

2.7. Analysis of cell viability

2.7.1. Measurement of combination index (CI)

The synergistic effect of Cisplatin and Tolf on A2780 cells was assessed with MTT method. Simply, cells were seeded at a density of 5×10^3 cells per well into 96-well plates. Overnight, the medium was removed and the cells were cultured with different doses of Cisplatin, Tolf and Tolf combined with Cisplatin for 24 h, respectively. Three duplicates were repeated for each group. Afterwards, each well was added with 20 μL of MTT solution (5 mg/mL) and incubated for 4 h in the sterile incubator. The medium was removed and 150 μL of dimethyl sulfoxide (DMSO) was added into each well. The plates were shaken for 10 min and put into the multifunction plate reader (Bio-RAD, USA) to measure the absorbance at 570 nm. IC_{50} was calculated by GraphPad Prism 9.0 software. CI value was calculated by the following formula: $CI=IC_{T+P} \times (1/IC_P + n/IC_T)$, where IC_{T+P}, IC_P and IC_T were the IC_{50} of Tolf combined with Cisplatin, Cisplatin, Tolf, respectively and n was the ratio of the concentration of Tolf to Cisplatin in the treatment groups of Tolf combined with Cisplatin.

2.7.2. Cytotoxicity assay

The same operations were as shown in "2.7.1" except that the A2780 cells were cultured with Cisplatin, Tolf, Tolf combined with Cisplatin, TNPs, PNPs, and TPNPs, respectively.

2.8. Cell apoptosis assay

FITC/PI Apoptosis Detection Kit was applied to detect the apoptosis of A2780 cells. Briefly, cells were seeded at a density of 4×10^5 cells per

well into 6-well plates. After incubated overnight, the cells were exposed to different treatment groups. The administration dosages were 5 μM Cisplatin and 20 μM Tolf. After 24 h, the cells were bound to fluorescent dyes in a standard procedure. Ultimately, flow cytometer (Becton-Dickinson FACS Calibur) was employed to analyze the prepared samples.

2.9. In vitro concentration of reactive oxygen species (ROS)

ROS level in A2780 cells was determined by flow cytometer and confocal laser scanning microscope (CLSM, Zeiss LSM 900). Firstly, A2780 cells were seeded at a density of 4×10^5 cells per well into 6-well plates and incubated for 24 h. Afterwards, the cells were treated for 4 h with the same doses of different formulations as shown in "2.8". Then, the cells were stained with fresh medium containing 2 μL DCFH-DA (10 mM) and incubated for 0.5 h. Finally, CLSM was used to take cell fluorescence images, and flow cytometry was applied to detect the fluorescence intensity.

2.10. Cell uptake

Cy5.5 was used to evaluate the intracellular status of free drug and nanomedicine. Primarily, Cy5.5-NPs were prepared by the following method. Cy5.5, LP, LT and DSPEG-PEG2000 were dissolved in DMF, the other preparation methods were the same as those in 2.4. Free Cy5.5 solution was prepared by diluting Cy5.5 dissolved in DMF into PBS. The final concentration of Cy5.5 was 0.2 mg/mL. Then A2780 cells were seeded in 6-well plates as shown in "2.8" and cultured overnight. Subsequently, 15 μL Cy5.5-NPs and free Cy5.5 solution were added into medium and incubated for 1.5 h, respectively. After that, PBS was used to clean the cells and fixed them for 15 min with 4% paraformaldehyde. Then the nucleus was stained with Hoechst reagent for 10 min. Ultimately, the fluorescent intensity of cells was imaged by CLSM.

2.11. Analysis of western blot (WB)

The expression of γ-H2AX, Caspase 3, p53 and Bcl-2 were semi-quantified by WB assay. Simply, A2780 cells were seeded at a density of 1×10^6 cells per well into 6-well plates and incubated overnight. Then the cells were exposed to different formulations. The dose of Cisplatin was 10 μM and the dose of Tolf was 40 μM. After 24 h, the cells were collected and proteins were extracted and quantified in accordance with the standard procedure. Following the standard procedure of WB, protein bands were revealed by enhanced chemiluminescence (ECL) detecting reagents, and photographed by the Image Analysis System (Protein Simple, USA). The gray value of the strip was analyzed by Image J software.

2.12. Hemolysis assay

The hemolysis test was used to evaluate the safety of drugs *in vivo*. First, 0.5 mL blood was taken from the eye corner venous plexus of mice and centrifuged at 4 °C at 1500 g for 10 min. The sediment was cleaned three times with 0.9% NaCl solution and formulated into a 2% erythrocyte suspension. 0.5 mL formulations and 0.5 mL erythrocyte suspension were co-incubated in 1.5 mL centrifuge tubes at 37 °C for 3 h. The dose of Cisplatin was 0.6 mM and the dose of Tolf was 2.4 mM. Then the centrifuge tubes were centrifuged at 1500 g for 10 min at 4 °C and photographed. 100 μL supernatant was absorbed into 96-well plate and the plate was put into the multifunction plate reader to measure the absorbance at 570 nm. Three duplicates were repeated for each group.

2.13. Fluorescence imaging in vivo

Cy5.5 was applied to visualize the difference of free drug and formulations on the tissue distribution *in vivo*. The PDX tumor blocks were implanted into the back of BALB/c mice subcutaneously. When the tumor grew to about 200 mm^3, 200 μL of free Cy5.5 and Cy5.5-NPs were injected into the mice via the tail vein. When the predetermined time (4, 8, 12, 24 h) was arrived, the mice were anesthetized by inhaling isoflurane and placed in an *in vivo* imaging system (IVIS Spectrum, Caliper, USA) to acquire the fluorescence imaging results. Finally, mice were sacrificed. The tumors and capital organs were dissected, rinsed with saline, blotted with filter paper and photographed.

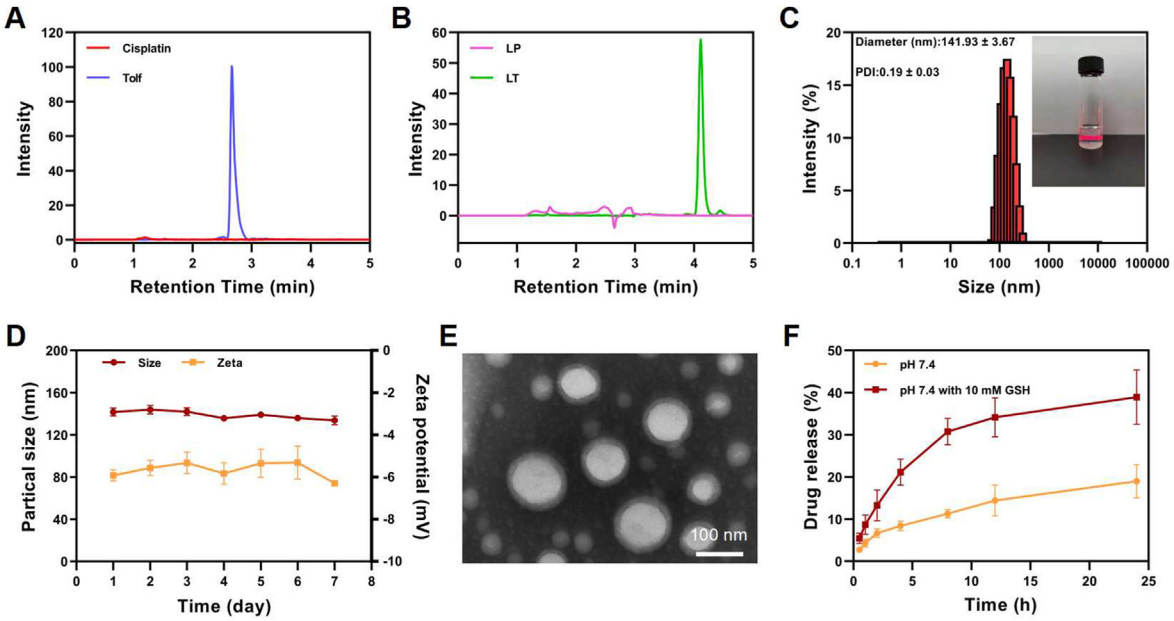

Fig. 1. Characterization of TPNPs. (A) Chromatograms of Cisplatin and Tolf (290 nm, 10% H_2O with 90% Acetonitrile). (B) Chromatograms of LP and LT (290 nm, 10% H_2O with 90% Acetonitrile). (C) Diameter distribution of TPNPs measured by DLS and appearance under laser beam. (D) Stability of TPNPs dispersed in PBS at room temperature. (E) TEM image of TPNPs (Scale bar: 100 nm). (F) Release of Tolf from TPNPs at pH 7.4 with or without 10 mM GSH (mean ± SD, n = 3).

2.14. Antitumor efficacy in vivo

The antitumor activity was estimated in the BALB/c nude mice bearing ovarian cancer PDX tumors. These mice bearing with ovarian cancer PDX models were stochastically divided into 7 groups with 5 mice each when the tumor grew to 100–200 mm^3. Then they were treated with different formulations, at the dosage of 2 mg/kg Cisplatin and 6.5 mg/kg Tolf. The administration cycle was once every 3 days, and the way of administration was intravenous. Meanwhile, body weights were recorded and the longest (a) and shortest (b) diameter of tumor were measured. The volume of the tumor was calculated as shown below formula: $V = 0.5 \times ab^2$. After five treatments, blood serum was collected, and the mice were sacrificed. Ultimately, tumors were dissected, rinsed with saline, blotted with filter paper, weighed and photographed.

2.15. Immunohistochemistry and immunofluorescence staining analysis

The main organs (heart, liver, spleen, lung, kidney) and tumors were removed after treatment, and soaked in 4% paraformaldehyde for further hematoxylin eosin (HE) staining. The immunofluorescence analysis of COX-2, *E*-cadherin, CD34 and Ki67 in tumor tissues was performed according to the standard procedures.

2.16. Serum biochemical analysis

The serum biochemical indexes were measured to evaluate the toxicity of drugs *in vivo*. The liver enzyme level was reflected by aminotransferase (AST) and alanine aminotransferase (ALT), and the renal function was evaluated by creatinine (CRE) and blood urea

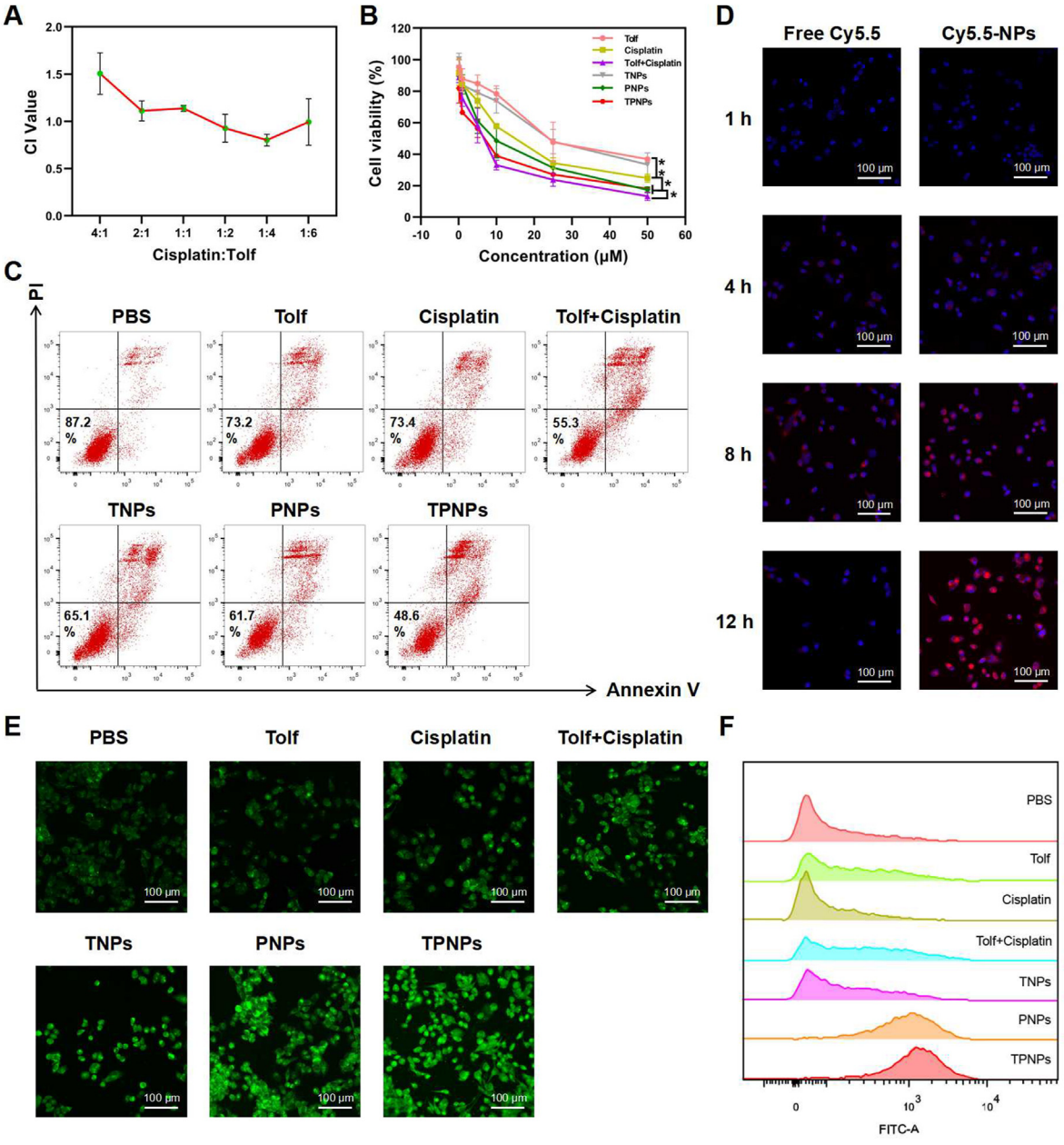

Fig. 2. *In vitro* cell assays. (A) The CI values of the combination of Tolf and Cisplatin in various proportions. (B) Cytotoxicity of different agents in variety concentration, *$p < 0.05$, **$p < 0.01$. (C) The apoptosis levels of A2780 cells treated with 5 μM Cisplatin and 20 μM Tolf for 24 h. (D) Cellular uptake of Cy5.5-NPs (15 μL, 0.2 mg/mL) and free drug (Scale bar: 100 μm). (E) Determination of intracellular ROS contents in A2780 cells with different drugs treatment for 4 h (Scale bar: 100 μm). (F) Fluorescence intensity of ROS treated with 5 μM Cisplatin and 20 μM Tolf for 4 h was determined by flow cytometry.

nitrogen (BUN). All of the indexes were assessed with the AU5800 Automatic Biochemical Analyzer (Beckman Coulter, USA).

3. Results and discussion

3.1. Synthesis and characterization of TPNPs

As previously reported, LP and LT were synthesized by esterification reaction [17]. The specific synthesis routes were shown in Fig. S1. The yield of LT (475 mg, 38%) was lower than that of LP (877 mg, 61%) because of the two-step esterification reaction in which the disulfide bond sensitive to GSH was bonded in the middle. Two resulting compounds were unambiguously characterized by ^{1}H NMR and high-resolution mass spectrometry (Figs. S2–S5). After successful synthesis, the RP-HPLC assay methods for Tolf and LT were developed. As shown in Fig. 1A–B, the retention time of Tolf and LT was different, and Cisplatin and LP did not interfere with their quantification. Then we dissolved the prodrug mixture in DMF and quickly added it to water to investigate the self-assembly capability. The average particle size of TPNPs, TNPs and PNPs was 142 nm, 129 nm and 104 nm, respectively (Fig. 1C, S6A, S7A). The morphology under the microscope of three NPs were uniformly spherical, and the sizes were consistent with those measured by the dynamic light scattering (DLS) (Fig. 1E, S6B, S7B). The particle size of NPs were so suitable that allowed them to be accumulated to the tumor site by the EPR effects [33]. The particle size of TPNPs could remain about 140 nm for a week and the zeta potential was maintained at - 6 mV (Fig. 1D), which could avoid hemolysis problems and safety problems caused by positive potential [34,35]. Furthermore, the encapsulation efficiency (EE) and drug loading (DL) of Cisplatin in TPNPs was 85.62 ± 1.31% and 8.62 ± 0.42%, and the EE and DL of Tolf in TPNPs was 82.41 ± 1.60% and 26.89 ± 0.60%, respectively. Similarly, the encapsulation efficiency (EE) and drug loading (DL) of Cisplatin in PNPs was 88.68 ± 1.81% and 27.01 ± 0.12%, and the EE and DL of Tolf in TNPs was 86.62 ± 0.60% and 35.92 ± 0.14%, respectively. Although the drug loadings appeared to vary widely, the concentration of the drug remained roughly the same. Subsequently, we further explored the release of LT and LP *in vitro* with or without GSH. The amount of Tolf and Pt of TPNPs with GSH after released 24 h was about 2 times of that without GSH (Fig. 1F, S8), which made it possible for TPNPs to be rapidly released when there was a high level of GSH in tumor, and to decrease the damage to normal tissues. Compared with TPNPs, the Tolf cumulative release of 24 h in TNPs increased by 7% and 5%, respectively, in the release media with or without GSH (Fig. S6C). Additionally, the Pt cumulative release of 24 h in PNPs increased by 5% and 3%, respectively, in the release media with or without GSH compared with TPNPs (Fig. S7C). Therefore, we can conclude that the three nanoparticles have similar physical and chemical properties and the prodrugs respond to tumor microenvironment are likely to play a synergistic and attenuated role.

3.2. Anti-tumor activity in vitro

Firstly, we determined the CI value of Tolf and Cisplatin in order to

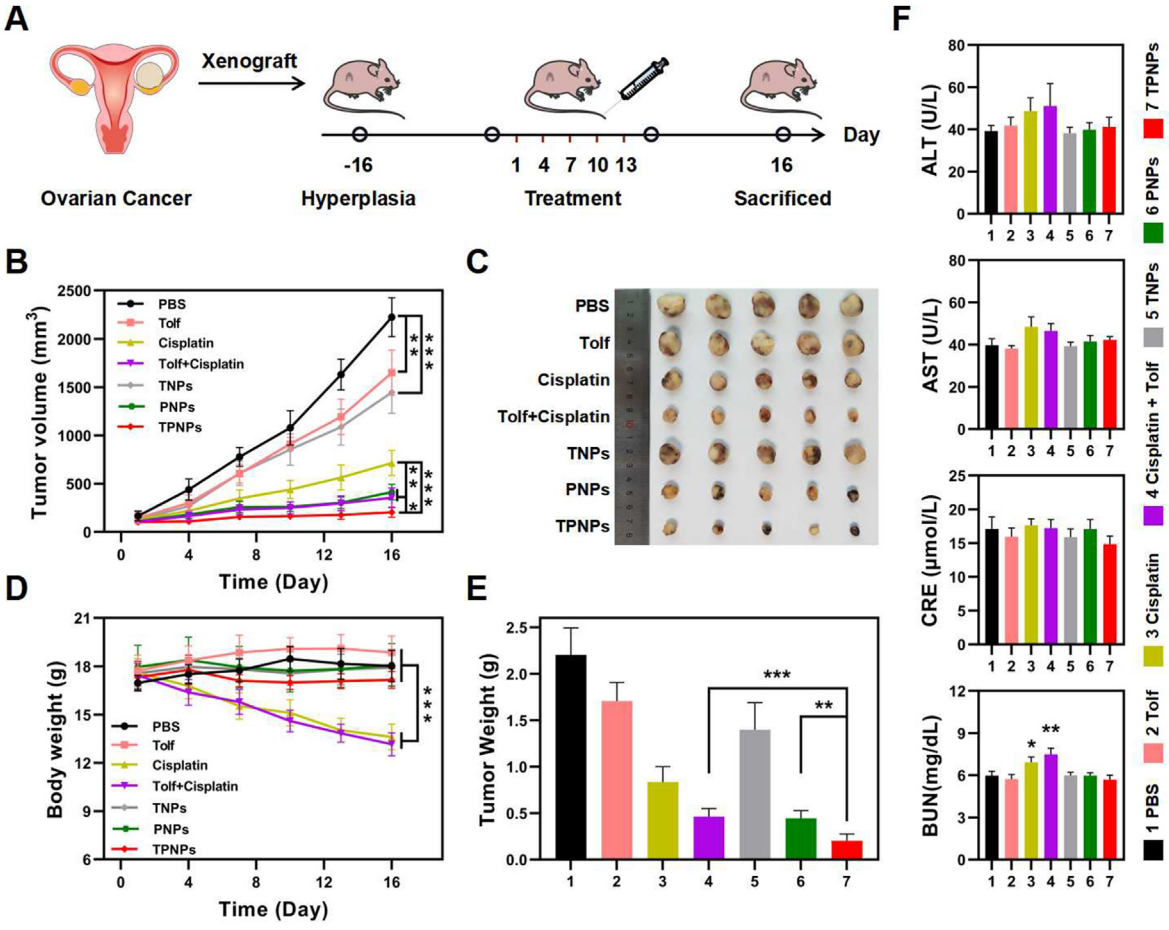

Fig. 3. *In vivo* distribution of Cy5.5-NPs and free Cy5.5 in the nude mice bearing ovarian cancer PDX tumors. (A) Live imaging of nude mice after injected with free Cy5.5 or Cy5.5-NPs intravenously (200 μL, 0.2 mg/mL). (B) *Ex vivo* imaging of normal tissues and tumors. (C) Semi-quantitative data of tumor signals in live mice at different time points. (D) Semi-quantitative data of signals in organs and tumor *in vitro*. (*p < 0.05, **p < 0.01, ***p < 0.001, between Cy5.5-NPs group and free Cy5.5 group).

obtain optimal therapeutic effect. The results revealed that the optimum anti-proliferation effect generated when the ratio of Cisplatin to Tolf was 1:4 (Fig. 2A). Therefore, TPNPs was prepared to treat ovarian cancer according to this mixing ratio. Then, we studied the antitumor effects of TPNPs on A2780 cells *in vitro*. As shown in Fig. 2B, the cell survival rates in each group were dose-dependent. After the drugs were made into NPs, the IC_{50} values of Tolf, Cisplatin and Tolf combined with Cisplatin changed from 32.37 μM, 13.55 μM, 5.10 μM–25.91 μM, 8.52 μM, 4.17 μM, respectively. The apoptosis assay was used to further verify the anti-proliferation effects of various formulations on A2780 cells. The percentage of apoptosis in NPs groups remarkably increased compared to the free drug groups and Tolf and Cisplatin showed obvious synergistic effect (Fig. 2C, S9). This result was consistent with that of MTT assay and we speculated that it might be caused by different cellular uptake of NPs and free drugs by A2780 cells. Therefore, Cy5.5-NPs were prepared and the cellular uptake was semi-quantified by CLSM. The fluorescence intensity of intracellular Cy5.5-NP was higher than that of free Cy5.5 at all the time points, especially at 8 h and 12 h (Fig. 2D). The time point of the strongest fluorescence intensity in the Cy5.5-NPs treated group was later than that in the free Cy5.5 treated group, which might be caused by the difference in uptake routes. Simultaneously, most chemotherapy drugs would cause the increase of ROS level in cells, and then promote cell apoptosis [36]. The results presented by fluorescence images (Fig. 2E, S10) and flow cytometry (Fig. 2F) showed that the ROS levels of the groups treated with NPs were significantly increased, which was consistent with the results of cell apoptosis. These results suggested a synergistic effect between Tolf and Cisplatin. In addition, after prepared to NPs, the increase of intracellular drug concentration and oxidative stress reaction caused increased apoptosis together.

3.3. *In vivo and ex vivo imaging*

In order to investigate the distribution of NPs in mice, the fluorescence imaging of Cy5.5-NPs and free Cy5.5 in BALB/c mice bearing ovarian cancer PDX tumors was compared by the *in vivo* imaging system. After 4 h intravenously, the fluorescent intensity of Cy5.5-NPs was not significantly different from that of free Cy5.5. Then the Cy5.5-NPs group showed slower metabolism and greater tumor accumulation efficiency compared to the free Cy5.5 group with the extension of time (Fig. 3A). This was more clearly complemented by semi-quantitative fluorescence data from tumors in live mice (Fig. 3C), which indicate that NPs could be efficiently transferred to the tumor site and might play a better role in tumor treatment than free drugs. Furthermore, the fluorescence imaging results of normal tissue and tumor showed that Cy5.5-NPs was more accumulative in lung and tumor tissue (Fig. 3B). In heart, liver, spleen, lung, kidney and tumor, the fluorescence intensity of the Cy5.5-NPs group was 2.11, 3.98, 1.89, 1.69, 2.02, 1.86 times that of the free Cy5.5 group (Fig. 3D). This might be caused by slow metabolism of Cy5.5-NPs *in vivo* and increased phagocytic uptake of the Reticuloendothelial System (RES) [37]. The above results indicated that the liver

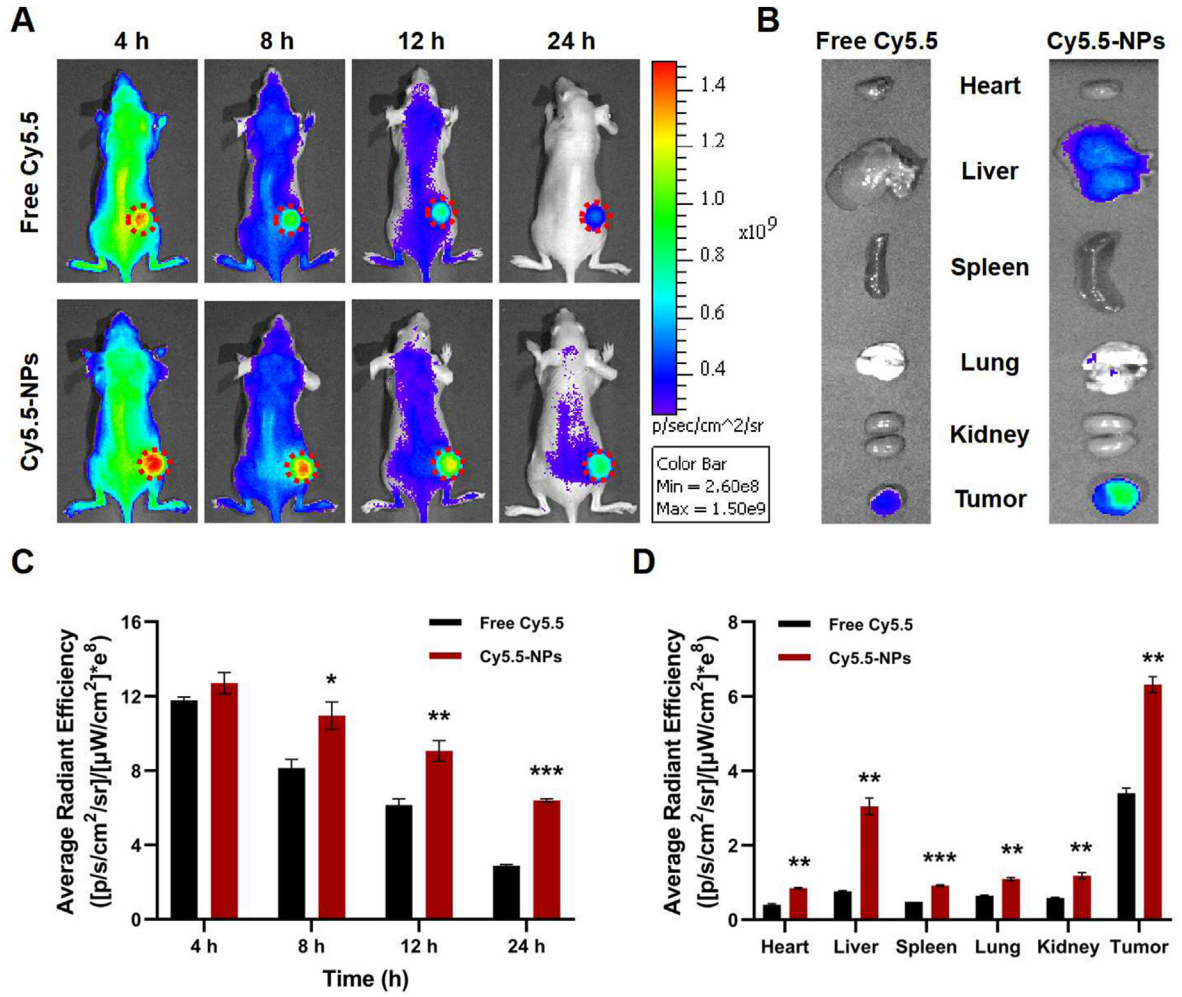

Fig. 4. *In vivo* antitumor efficacy. (A) Experimental flow chart in the nude mice bearing PDX tumors. (B) Growth curves of tumor volume after treated with 2 mg/kg Cisplatin and 6.5 mg/kg Tolf (n = 5, *p < 0.05, **p < 0.01, ***p < 0.001). (C) Tumor image. (D) Changes in Body weight (n = 5, ***p < 0.001). (E) Tumor weights (n = 5, **p < 0.01, ***p < 0.001). (F) ALT, AST, BUN and CRE levels in serum. (Mean ± SD, *p < 0.05, **p < 0.01).

metabolic pathway and the *in vivo* circulation time increased after prepared into NPs, indicating that the *in vivo* antitumor efficacy test may have a satisfactory result.

3.4. Antitumor efficacy in vivo

The hemolysis experiment was conducted first to confirm the biosecurity of NPs and free drugs. As shown in Fig. S11, there was no obvious hemolysis occurred in all preparations after co-incubation with red blood cell suspension. The hemolysis rates of NPs were decreased compared with free drugs, which indicated that the safety of NPs had been improved. Subsequently, the *in vivo* antitumor activity was examined in the nude mice bearing PDX tumors. Different preparations were administered every 3 days through a caudal vein for a total of 5 treatments (Fig. 4A). As shown in Fig. 4B, the curves of tumor volume revealed that the therapeutic effect of NPs were better than that of free drugs and it was obvious that the TPNPs treatment group had the smallest tumor volume after the treatment, about 204 mm^3. The therapeutic effects of prodrug NPs were increased compared with free drugs. After treatment, the tumor tissue was dissected, photographed (Fig. 4C) and weighed (Fig. 4E). After preparation of prodrug NPs, the tumor inhibition rates of Tolf, Cisplatin, and mixture of Tolf and Cisplatin increased from 23%, 62%, 79% to 36, 80%, 91%, respectively. This showed that Tolf and Cisplatin have a significant synergistic antitumor effect and a better therapeutic effect of prodrug NPs, which may be related to the fact that NPs accumulate more at the tumor site than free drugs. Furthermore, the curves of body weights suggested that the TPNPs group did not cause weight change (Fig. 4D), indicating that TPNPs had almost no toxicity to ovarian cancer treatment, whereas the mice given Cisplatin and the mixture of dual drugs had a significant reduction in body weight. Moreover, the biosecurity of TPNPs was also confirmed by H&E staining on different organs and biochemical indexes, while free Cisplatin and

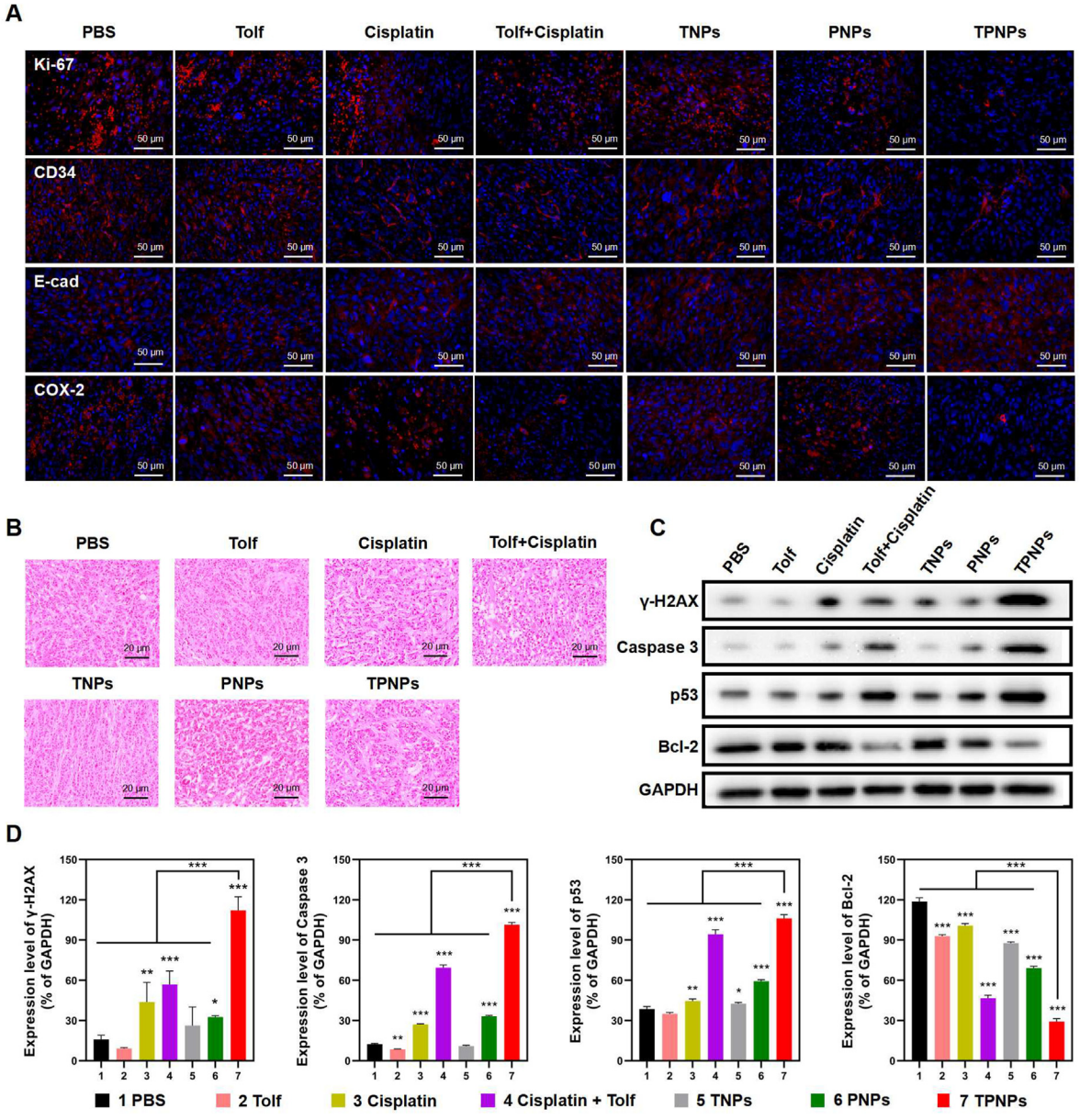

Fig. 5. The mechanism of antitumor effect. (A) Fluorescence intensity of Ki-67 staining and the expression of CD34, *E*-cadherin and COX-2 in the tumor tissues of mice after treatment (Scale bar: 50 μm). (B) Histological analysis of tumor (Scale bar: 20 μm). (C) Western blotting analysis of γ-H2AX, Caspase 3, p53 and Bcl-2 in A2780 cells after treated with 5 μM Cisplatin and 20 μM Tolf for 24 h. (D) The semi-quantitative analysis of γ-H2AX, Caspase 3, p53 and Bcl-2 expression levels, $^*p < 0.05$, $^{**}p < 0.01$, $^{***}p < 0.001$.

mixture of Tolf and Cisplatin caused some damage to the mouse kidney (Fig. 4F, S12). Taken together, free Cisplatin metabolized by the kidney may cause kidney damage, while Tolf did not increase the side effect of Cisplatin on kidney, indicating its high safety. Compared with free drugs, NPs have achieved the function of enhancing efficacy and reducing toxicity, which has a promising clinical application prospect.

3.5. Antitumor mechanism study

To detect apoptosis in tumors, we first detected the expression of Ki-67, CD34 and *E*-cadherin using immunofluorescence (Fig. 5A) and H&E staining of tumors (Fig. 5B). Compared with other preparations, TPNPs could significantly induce tumor cell apoptosis. As markers of neovascularization, CD34 and *E*-cadherin are closely related to tumor cell invasion and metastasis. The results of decreased CD34 expression and increased *E*-cadherin expression indicated that TPNPs can significantly inhibit tumor growth, which were consistent with the results of antitumor activities *in vivo*. COX-2 levels within tumors were further detected to verify whether TPNPs had the same or enhanced inhibitory effect on COX-2 expression as Tolf. As illustrated in Fig. 5A, the level of COX-2 in the TPNPs treated group was the lowest compared with other groups, which indicated that TPNPs enhanced the inhibition of COX-2 expression in tumor. It has been reported that the inhibition of COX-2 could rise the expression of p53, which was critical for apoptosis pathways [38,39]. Therefore, we detected the expression of several relevant proteins in A2780 cells after different preparations treatment. As illustrated in Fig. 5C and D, the expression of p53 in TPNPs treated group was significantly increased. Then the higher p53 expression down-regulated the Bcl-2 expression and promoted apoptosis. γ-H2AX was a marker of DNA damage [40] and Caspase 3 was a marker of mitochondrial damage [41,42]. The expression level of γ-H2AX and Caspase 3 indicated that TPNPs induced apoptosis both through induced DNA breakage and endogenous mitochondrial pathway. In conclusion, TPNPs could simultaneously exert Tolf to inhibit COX-2 expression and cisplatin-induced DNA damage and mitochondrial damage, playing a synergistic anti-tumor role.

4. Conclusions

In summary, we report a Cisplatin and Tolf based prodrug self-assembled nanoparticles for the treatment of ovarian cancer. TPNPs has a high drug loading capacity, and its uptake by tumor cells was significantly enhanced both *in vivo* and *in vitro*. After reaching the tumor site through passive targeting, free drugs can be dissociated under high GSH conditions in the tumor microenvironment. Cisplatin rapidly attached to DNA in nucleus, resulting in DNA damage and mitochondria damage. Simultaneously, Tolf could suppress COX-2 expression and cooperate with Cisplatin in antitumor. TPNPs has shown effective therapeutic efficacy and lower toxicity than free Cisplatin in the mice xenograft model of human ovarian cancer, which have great clinical application prospects.

Author contributions

Xiao Ma: Investigation, Software, Methodology, Formal analysis, Writing – original draft. Yangjia Liu: Software, Validation, Formal analysis, Data curation, Writing – original draft. Hanmei Wu: Software, Validation. Jinxiu Tan: Formal analysis, Data curation. Wenying Yi: Software, Data curation. Zhenjie Wang: Supervision, Writing – review & editing. Zhiqiang Yu: Supervision, Resources. Xuefeng Wang: Conceptualization, Project administration, Resources.

Declaration of competing interest

The authors declare that they have no known competing financial interests or personal relationships that could have appeared to influence the work reported in this paper

Data availability

Data will be made available on request.

Acknowledgements

We are grateful for financial support from GDNRC (Guangdong nature resource center) [grant number (2020)037] and Natural Science Foundation of Guangdong Province [grant number 22019A1515011498, 2019A1515011619]. We also wish to acknowledge the support of the Institute of Applied Chemistry of CAS and the Animal Laboratory Center of Southern Medical University.

Appendix A. Supplementary data

Supplementary data to this article can be found online at https://doi.org/10.1016/j.mtbio.2023.100698.

References

[1] S. Sambasivan, Epithelial ovarian cancer: review article, Cancer Treat. Res. Commun. 33 (2022), 100629.
[2] S. Ghosh, Cisplatin: the first metal based anticancer drug, Bioorg. Chem. 88 (2019), 102925.
[3] A.S. Abu-Surrah, M. Kettunen, Platinum group antitumor Chemistry: design and development of new anticancer drugs complementary to cisplatin, Curr. Med. Chem. 13 (2006) 1337–1357.
[4] J. Wang, G.S. Wu, Role of autophagy in Cisplatin resistance in ovarian cancer cells, J. Biol. Chem. 289 (2014) 17163–17173.
[5] A. Arakawa, H. Nishikawa, M. Sugiura, Paclitaxel/carboplatin/cyclooxygenase-2 inhibitor as first-line chemotherapy in ovarian cancer and endometrial cancer, Nagoya Med. J. 50 (2009) 31–36.
[6] S.A. Aldossary, Review on pharmacology of cisplatin: clinical use, toxicity and mechanism of resistance of cisplatin, Biomed. Pharmacol. J. 11 (2019) 7–15.
[7] Z. Herrera-Pérez, N. Gretz, H. Dweep, A comprehensive review on the genetic regulation of cisplatin-induced nephrotoxicity, Curr. Genom. 17 (2016) 279–293.
[8] P. Aishwarya, M. Sandhya, R.V. Chidrawar, V. Uma, M. Rao, A review on gender related effects of Cisplatin induced nephrotoxicity, Int. J. Invent. Pharm. Sci. 2 (2014) 591–595.
[9] P. Zhang, Y. Xiao, X. Sun, X. Lin, S. Koo, A.V. Yaremenko, D. Qin, N. Kong, O.C. Farokhzad, W. Tao, Cancer nanomedicine toward clinical translation: obstacles, opportunities, and future prospects, Méd. 4 (2022) 147–167.
[10] A. Xie, S. Hanif, J. Ouyang, Z. Tang, N. Kong, N.Y. Kim, B. Qi, D. Patel, B. Shi, W. Tao, Stimuli-responsive prodrug-based cancer nanomedicine, EBioMedicine 56 (2020), 102821.
[11] N. Kong, R. Zhang, G. Wu, X. Sui, J. Wang, N.Y. Kim, S. Blake, D. De, T. Xie, Y. Cao, W. Tao, Intravesical delivery of KDM6A-mRNA via mucoadhesive nanoparticles inhibits the metastasis of bladder cancer, Proc. Natl. Acad. Sci. U.S.A. 119 (2022), e2112696119.
[12] L. Yu, M. Yu, W. Chen, S. Sun, W. Huang, T. Wang, Z. Peng, Z. Luo, Y. Fang, Y. Li, Y. Deng, M. Wu, W. Tao, In situ separable nanovaccines with stealthy bioadhesive capability for durable cancer immunotherapy, J. Am. Chem. Soc. 145 (2023) 8375–8388.
[13] J. Ouyang, A. Xie, J. Zhou, R. Liu, L. Wang, H. Liu, N. Kong, W. Tao, Minimally invasive nanomedicine: nanotechnology in photo-/ultrasound-/radiation-/magnetism-mediated therapy and imaging, Chem. Soc. Rev. 51 (2022) 4996–5041.
[14] Y. Han, P. Wen, J. Li, K. Kataoka, Targeted nanomedicine in Cisplatin-based cancer therapeutics, J. Contr. Release 345 (2022) 709–720.
[15] Y. Yang, Z. Mai, Y. Zhang, Z. Yu, W. Li, Y. Zhang, F. Li, P. Timashev, P. Luan, D. Luo, X.-J. Liang, Z. Yu, A cascade targeted and mitochondrion-dysfunctional nanomedicine capable of overcoming drug resistance in hepatocellular carcinoma, ACS Nano 17 (2023) 1275–1286.
[16] Y. Yang, Y. Yu, H. Chen, X. Meng, W. Ma, M. Yu, Z. Li, C. Li, H. Liu, X. Zhang, H. Xiao, Z. Yu, Illuminating platinum transportation while maximizing therapeutic efficacy by gold nanoclusters via simultaneous near-infrared-I/II imaging and glutathione scavenging, ACS Nano 14 (2020) 13536–13547.
[17] H. Wang, Z. Lu, L. Wang, T. Guo, S. Zheng, New generation nanomedicines constructed from self-assembling small molecule prodrugs alleviate cancer drug toxicity, Cancer Res. 77 (2017) 6963–6974.
[18] T. Ronny, R. Worranan, S. Warayuth, K.V. Mont, O. Praneet, T. Prasopchai, Chitosan-based self-assembled nanocarriers coordinated to Cisplatin for cancer treatment, RSC Adv. 8 (2018) 22967–22973.
[19] Z. Mai, J. Zhong, J. Zhang, G. Chen, Y. Tang, W. Ma, G. Li, Z. Feng, F. Li, X.-J. Liang, Y. Yang, Z. Yu, Carrier-free immunotherapeutic nano-booster with dual synergistic effects based on glutaminase inhibition combined with photodynamic therapy, ACS Nano 17 (2023) 1583–1596.

[20] X. Yu, Y. Yang, H. Yuan, M. Wu, S. Li, W. Gong, J. Yu, W. Xia, Y. Zhang, G. Ding, Inhibition of COX-2/PGE2 cascade ameliorates Cisplatin-induced mesangial cell apoptosis, Am. J. Transl. Res. 9 (2017) 1222–1229.
[21] R. Ali-Fehmi, M. Che, I. Khalifeh, J.M. Malone, R. Morris, W.D. Lawrence, A.R. Munkarah, The effect of cyclooxygenase-2 expression on tumor vascularity in advanced stage ovarian serous carcinoma, Cancer 98 (2003) 1423–1429.
[22] J.-Y. Lee, S.-K. Myung, Y.-S. Song, Prognostic role of cyclooxygenase-2 in epithelial ovarian cancer: a meta-analysis of observational studies, Gynecol. Oncol. 129 (2013) 613–619.
[23] F. Guo, J. Tian, Y. Jin, L. Wang, R. Yang, Effects of cyclooxygenase-2 gene silencing on the biological behavior of SKOV3 ovarian cancer cells, Mol. Med. Rep. 11 (2015) 59–66.
[24] F. Wang, H. Zhang, A.H. Ma, W. Yu, M. Zimmermann, J. Yang, S.H. Hwang, D. Zhu, T.Y. Lin, M. Malfatti, COX-2/sEH dual inhibitor PTUPB potentiates the antitumor efficacy of cisplatin, Mol. Cancer Therapeut. 17 (2017) 474–483.
[25] R. Basha, C.H. Baker, U.T. Sankpal, S. Ahmad, S. Safe, J.L. Abbruzzese, M. Abdelrahim, Therapeutic applications of NSAIDS in cancer: special emphasis on tolfenamic acid, Front. Biosci. 3 (2011) 797–805.
[26] R. Basha, S.B. Ingersoll, U.T. Sankpal, S. Ahmad, C.H. Baker, J.R. Edwards, R.W. Holloway, S. Kaja, M. Abdelrahim, Tolfenamic acid inhibits ovarian cancer cell growth and decreases the expression of c-Met and survivin through suppressing specificity protein transcription factors, Gynecol. Oncol. 122 (2011) 163–170.
[27] J. Jeong, X. Yang, R. Clark, J. Choi, S. Baek, S. Lee, A mechanistic study of the proapoptotic effect of tolfenamic acid: involvement of NF-κB activation, Carcinogenesis 34 (2013) 2350–2360.
[28] U.T. Sankpal, S.B. Ingersoll, S. Ahmad, R.W. Holloway, V.B. Bhat, J.W. Simecka, L. Daniel, E. Kariali, J.K. Vishwanatha, R. Basha, Association of Sp1 and survivin in epithelial ovarian cancer: sp1 inhibitor and Cisplatin, a novel combination for inhibiting epithelial ovarian cancer cell proliferation, Tumor Biol. 37 (2016) 14259–14269.
[29] U.T. Sankpal, G.P. Nagaraju, S.R. Gottipolu, M. Hurtado, C.G. Jordan, J.W. Simecka, M. Shoji, B.E. Rayes, R. Basha, Combination of Tolfenamic acid and curcumin induces colon cancer cell growth inhibition through modulating specific transcription factors and reactive oxygen species, Oncotarget 7 (2016) 3186–3200.
[30] D. Kovala-Demertzi, D. Hadjipavlou-Litina, A. Primikiri, M. Staninska, C. Kotoglou, M. Demertzis, A. Anti-inflammatory, antiproliferative, and radical-scavenging activities of tolfenamic acid and its metal complexes, Chem. Biodiversity 6 (2010) 948–960.
[31] C.X. Yang, L. Xing, X. Chang, T.J. Zhou, Y.Y. Bi, Z.Q. Yu, Z.Q. Zhang, H.L. Jiang, Synergistic platinum(II) prodrug nanoparticles for enhanced breast cancer therapy, Mol. Pharm. 17 (2020) 1300–1309.
[32] L. Xing, C.X. Yang, D. Zhao, L.J. Shen, H.L. Jiang, A carrier-free anti-inflammatory platinum (II) self-delivered nanoprodrug for enhanced breast cancer therapy, J. Contr. Release 331 (2021) 460–471.
[33] Upreti Meenakshi, Jyoti Amar, Sethi Pallavi, Tumor microenvironment and nanotherapeutics, Transl. Cancer Res. 2 (2013) 309–319.
[34] M. Manaargadoo-Catin, A. Ali-Cherif, J.L. Pougnas, C. Perrin, Hemolysis by surfactants - a review, Adv. Colloid Interface Sci. 228 (2015) 1–16.
[35] N. Lomeli, K. Di, J. Czerniawski, J.F. Guzowski, D.A. Bota, Cisplatin-induced mitochondrial dysfunction is associated with impaired cognitive function in rats, Free Radic. Biol. Med. 102 (2017) 274–286.
[36] S. Wang, K. Yu, Z. Yu, B. Zhang, C. Chen, L. Lin, Z. Li, Z. Li, Y. Zheng, Z. Yu, Targeting self-enhanced ROS-responsive artesunatum prodrug nanoassembly potentiates gemcitabine activity by down-regulating CDA expression in cervical cancer, Chin. Chem. Lett. 34 (2023), 108184.
[37] S. Chono, T. Tanino, T. Seki, K. Morimoto, Uptake characteristics of liposomes by rat alveolar macrophages: influence of particle size and surface mannose modification, J. Pharm. Pharmacol. 59 (2010) 75–80.
[38] C.A. Corcoran, Q. He, Y. Huang, M.S. Sheikh, Cyclooxygenase-2 interacts with p53 and interferes with p53-dependent transcription and apoptosis, Oncogene 24 (2005) 1634–1640.
[39] E.M. Choi, J.I. Heo, J.Y. Oh, Y.M. Kim, K.S. Ha, J.I. Kim, J.A. Han, COX-2 regulates p53 activity and inhibits DNA damage-induced apoptosis, Biochem. Biophys. Res. Commun. 328 (2005) 1107–1112.
[40] C. Bañuelos, J. Banáth, J. Kim, C. Aquino-Parsons, P. Olive, Gamma H2AX expression in tumors exposed to Cisplatin and fractionated irradiation, Clin. Cancer Res. 15 (2009) 3344–3353.
[41] M. Brentnall, L. Rodriguez-Menacol, R.L.D. Guevara, E. Cepero, L.H. Boise, Caspase-9, caspase-3 and caspase-7 have distinct roles during intrinsic apoptosis, BMC Cell Biol. 14 (2013) 32.
[42] Kishino Hayashi, Maeda Jike, Oshima, Caspase-8 regulates endoplasmic reticulum stress-induced necroptosis independent of the apoptosis pathway in auditory cells, Int. J. Mol. Sci. 20 (2019) 5896.